Catalysis Letters 18 (1993) 15–26

# Oxidative coupling of methane. The effect of alkali chlorides on molybdate based catalyst leading to high selectivity in $C_3$-product formation

John Kiwi[1], K. Ravidranathan Thampi, N. Mouaddib, Michael Grätzel
*Institut de Chimie Physique, Ecole Polytechnique Fédérale de Lausanne,*
*CH-1015 Lausanne, Switzerland*

and

Peter Albers
*Degussa AG, Abt. FC Ph, D-6540 Wolfgang Hanau, Germany*

Received 29 September 1992; accepted 12 January 1993

LiCl–$Na_2MoO_4$ was found to be an active catalyst for oxidative coupling of methane at temperatures around 620°C. In these systems, the selectivity for the formation of $C_3$-products exceeds the selectivity for the formation of $C_2$-products. While the homogeneous reaction of $CH_4$ and $O_2$ leads to $C_3H_6$ as $C_3$-product, the 50% LiCl–50% $Na_2MoO_4$ catalyst leads to $C_3H_8$ as the predominant $C_3$-product, indicating that in the latter case the reaction cannot be purely homogeneous. The dependency of the product distribution on temperature, gas composition, reactor dimensions, flow rate, $CH_4/O_2$ ratio and type of catalyst has been studied. The reaction was studied by co-feeding $CH_4$, $O_2$ and a diluent gas at atmospheric pressure continuously in a conventional flow reactor containing the catalyst. The reaction products observed were: $C_2H_4$, $C_2H_6$, $C_3H_6$, $C_3H_8$, $H_2O$ and $CO + CO_2$. The two latter gases were the main oxidation products observed. Characterization of the catalysts used was carried out by X-ray photoelectron spectroscopy (XPS) and X-ray diffraction (XRD).

**Keywords:** Methane coupling; molybdate-sodium; lithium chloride; propylene; propane

## 1. Introduction

During the last decade, oxidative coupling of $CH_4$ has become an important area of catalytic research. Following the pioneering work of Keller and Bhasin [1], much research has been carried out in this field. Recent work has been reviewed

---

[1] To whom correspondence should be addressed.

by Hutchings et al. [2], Anderson [3] and Mackie [4]. Previous work in our laboratory with molybdate catalysts useful in $CH_4$ activation has produced mainly $C_2$-products [5,6].

This report shows the conditions and catalysts involved in $CH_4$ coupling leading to $C_3H_x$ production (propane and propylene). The aim of the study was to look into the various possibilities of converting $CH_4$ to a high value added product, through a low-cost one-step catalytic process. $C_3H_6$ and $C_3H_8$ are also very desirable reaction products, since they can be easily separated from $CH_4$ stream after oxidation, compared to $C_2H_4$ and $C_2H_6$. Arata et al. have observed the formation of $C_3$-hydrocarbons during methane dimerization catalyzed by $Na^+$ doped type catalysts [7]. From the mechanistic point of view, the production of $C_3H_x$ ($x = 6, 8$) may involve reaction between vinyl radicals $CH_2{=}CH\cdot$ with $CH_3\cdot$.

Oxidative methane conversion to $C_3H_x$ catalyzed by PbO, $PbSO_4$ [8] and several alkaline-earth oxides has been reported by Carreiro and Baerns [9]. The purpose of the present work is to explore the role of alkali chlorides in the production of $C_3$-products. Chlorine is well known to increase the selectivity of partial oxidation reactions, such as ethylene oxide from ethylene [10] and formaldehyde from methane [11]. Burch et al. [12,13] have shown that oxidative coupling carried out with chlorine-containing catalysts produces substantial amounts of ethylene. Work reported by that group in the last five years indicates that chlorine seems to block total oxidation sites on the surface of oxide catalysts (such as $MnO_2$), resulting in higher $SC_2$ (selectivity for $C_2$-products) values. It has been suggested that an important role of chlorine is to produce new active sites over the catalyst, that are selective to the activation of ethane rather than methane [14].

## 2. Experimental

The reactor was a quartz U-tube. The tube was 560 mm in length with 6 mm i.d. The fixed catalyst bed was held in position by quartz wool plugs. The reactor was operated in the single-pass mode. The first and last 7 cm of the reactor were outside the furnace, 42 cm were inside the furnace. The catalyst was situated in the second half of the U-tube. With 1.2 g catalyst, the free volume of the cell (on the average) was 15.8 $cm^3$. Always "new" quartz reactors were used for the empty reactor runs and in each of the additional series of experiments reported in tables 1, 2 and figs. 1, 2. Catalysts were prepared by mechanically mixing the pure molybdate compound and alkali chloride in each case.

The reaction was allowed to proceed for 2 h at each reaction temperature, before collecting the data with good reproducibility.

Product analysis was performed by gas chromatography (GC) using a thermal conductivity detector. The gases $CH_4, C_2H_4, C_2H_6, C_3H_6, C_3H_8$ and $CO_2$ were detected on a Porapak QS column at 60°C, using He as carrier gas in a Carlo Erba

HRGC 5300 Mega Series gas chromatograph. For CO and $O_2$ analysis, a molecular sieve 5 Å column at 40°C was used. The absence of $C_2H_2$ in the product stream was confirmed chromatographically by using a Porasil-B column. $H_2$ was analysed on a molecular sieve 5 Å column, using Ar as the carrier gas. Water produced during the reaction was trapped at the reactor exit. $C_3H_6$ was detected in the gap phase as well as in the liquid $H_2O$ collected in the trap. Small quantities of HCHO and $CH_3OH$ (less than 2%), were also observed (as reaction products) in both phases. Inlet gas flows were measured by calibrated flow meters. The activity of the catalysts is defined by the percentage conversion of $CH_4$ into all products. The selectivity $X$(i)% to product i is defined as the percentage amount of product i/amount of total reaction products.

The XPS-measurements were performed using a Leybold surface analyser equipped with a separate gas reaction cell attached to the spectrometer chamber. The base pressure of the spectrometer was $2 \times 10^{-10}$ mbar and during the measurements $8 \times 10^{-9}$ mbar. The XPS-spectra were recorded using a twin anode X-ray gun (Mg $K_\alpha$/Al $K_\alpha$) at a power of 200 and 250 W respectively, and a hemispherical energy analyzer (Leybold EA11/100). The spectrometer calibration was repeatedly performed, following and referencing to the Au $4f_{7/2}$-signal at 84.0 eV. X-ray powder diffraction patters were recorded from 0° to 90° (2O) using a Hijaku diffractometer. A relatively large X-ray beam, 5 mm in diameter, permitted analysis of large quantities of powder, providing structural information on the main phases of each sample. No BET surface area was measured since the catalyst is a mixture of two polycrystalline inorganic salts.

## 3. Results and discussion

Table 1 presents the variation in $C_2$- and $C_3$-selectivity ($SC_2$ and $SC_3$), $C_2$- and $C_3$-yield ($YC_2$ and $YC_3$), and $CH_4$-conversion ($C_{C_1}$) with change in temperature. The data on empty reactor run presents the homogeneous thermal reaction taking place when a flowing gas consisting of 7.5 ml/min $CH_4$, 8.5 ml/min $O_2$ and 14 ml/min He react in a relatively long (560 mm × 6 mm i.d.), empty reactor. The formation of $C_2$-products ($C_2H_4$ and $C_2H_6$) is important at the temperatures shown in table 1. In agreement with previous work, $CH_4$ can be dimerized through a homogeneous gas-phase reaction in the presence of oxygen [15–17]. An increase in $C_2$-selectivity up to 650°C was observed in the empty reactor results, reported in table 1. This shows that up to this temperature, the formation of methyl radicals increases, favouring $C_2$-formation [18,19]. It also shows that selectivity towards $C_2 + C_3$ products is about 26%, whilst the selectivity towards $CO + CO_2$ products is $>70\%$.

Numerous preliminary experiments varying the gas flow, ratio $CH_4/O_2$, reactor geometry and dimensions, and quantity of diluent gas added (He) were carried out in order to achieve the lowest selectivity towards the formation of $C_3$-products. In this way, the heterogeneously catalyzed contribution towards the $CH_4$ coupling

Table 1

Methane conversions, selectivities and yields (in %) of $C_2$- and $C_3$-products for various catalysts and temperatures used

| $T$(°C) | Empty reactor | | | | | 1.2 g $Na_2MoO_4$ | | | | | 0.6 g $Na_2MoO_4$ + 0.6 g NaCl | | | | | 0.6 g $Na_2MoO_4$ + 0.6 g LiCl | | | | |
|---|---|---|---|---|---|---|---|---|---|---|---|---|---|---|---|---|---|---|---|---|
| | $C_{C_1}$ | $SC_2$ | $SC_3$ | $YC_2$ | $YC_3$ | $C_{C_1}$ | $SC_2$ | $SC_3$ | $YC_2$ | $YC_3$ | $C_{C_1}$ | $SC_2$ | $SC_3$ | $YC_2$ | $YC_3$ | $C_{C_1}$ | $SC_2$ | $SC_3$ | $YC_2$ | $YC_3$ |
| 570 | 7.0 | 10 | 2.0 | 0.7 | 0.1 | 17 | 27 | – | 4.6 | – | 2.0 | 8.0 | – | 0.2 | – | 11 | 40 | 15 | 4.4 | 1.6 |
| 590 | 8.0 | 16 | 2.0 | 1.3 | 0.2 | 18 | 29 | – | 5.2 | – | 4.0 | 15 | – | 0.6 | – | 10 | 29 | 22 | 2.9 | 2.2 |
| 610 | 9.0 | 20 | 2.0 | 1.8 | 0.2 | 16 | 30 | – | 4.8 | – | 5.0 | 25 | – | 1.2 | – | 9.0 | 22 | 32 | 2.0 | 2.9 |
| 630 | 12 | 23 | 2.0 | 2.7 | 0.2 | 15 | 30 | – | 4.5 | – | 6.5 | 27 | – | 1.7 | – | 8.0 | 21 | 35 | 1.6 | 2.8 |
| 650 | 18 | 26 | 1.9 | 4.7 | 0.4 | 14 | 30 | – | 4.2 | – | 8.5 | 28 | – | 2.4 | – | 9.0 | 20 | 28 | 1.8 | 2.5 |
| 670 | 20 | 24 | 1.8 | 4.8 | 0.4 | 14 | 30 | – | 4.2 | – | 9.0 | 28 | – | 2.6 | – | 11 | 20 | 13 | 2.2 | 1.4 |
| 690 | 21 | 19 | 1.7 | 4.0 | 0.3 | 14 | 28 | 3.0 | 3.9 | 0.4 | 9.5 | 29 | 7.0 | 2.7 | 0.7 | 15 | 20 | 7.0 | 3.0 | 1.1 |
| 710 | 22 | 17 | 1.4 | 3.7 | 0.3 | 16 | 26 | 2.5 | 4.2 | 0.4 | 13 | 28 | 10 | 3.6 | 1.3 | 16 | 19 | 5.0 | 3.0 | 0.8 |
| 730 | 23 | 14 | 1.0 | 3.2 | 0.2 | 22 | 15 | 2.0 | 3.3 | 0.4 | 19 | 23 | 13 | 4.4 | 2.5 | 17 | 18 | 5.0 | 3.1 | 0.8 |

reaction could later be shown distinctively. In table 1, a residence time of about 31.6 s is maintained. The use of He as diluant was necessary to reduce the residence time for the two reactive gases, $CH_4$ and $O_2$ in the reaction tube. The $C_3$-product due to the homogeneous reaction consists only of $C_3H_6$. No temperatures higher than 730°C were applied since a steady decrease in the values of $SC_3$ and $YC_3$ beyond 740°C was observed with increasing temperature.

In table 1, experimental data shows that when using 1.2 g of $Na_2MoO_4$ as catalyst, $SC_2$ values of 30% are seen at 630°C as compared to an $SC_2$ value of 26% reported for an empty reactor at this temperature. $Na_2MoO_4$ is a dehydration and dehydrogenation agent in gas-phase reactions at temperatures above 450°C [20,21]. For $Na_2MoO_4$, a decrease in $C_2$-selectivities ($SC_2$) was observed at temperatures higher than 670°C. This could be due to liquifaction of the catalyst as it is transformed into molten phase at 687°C [22–24]. Furthermore, the long contact time of $C_2H_4$ and $C_2H_6$ at the low flow rates used, allowed the $C_2$- and $C_3$-products to be converted into CO and $CO_2$. High selectivity values observed for CO and $CO_2$ in these experiments seem to confirm this rationalization. For the homogeneous catalytic process in the absence of the catalyst $\approx$ 80% of $O_2$ in the feed stream gets consumed at 620°C. When the reactor contains 1.2 g catalyst $\approx$ 90% $O_2$ is consumed, confirming the observed increase in catalytic process taking place.

The data showing the conversions, selectivities and yields in a reactor using the same gas stream, but containing 0.6 g of $Na_2MoO_4$ and 0.6 g of NaCl as a function of temperature is shown next in table 1. It is seen that $SC_3$ values at all temperatures increase significantly over the values for $SC_3$ reported when using $Na_2MoO_4$ alone. $Li_2CO_3$ was tried, but was found to hinder the $C_3$-coupling reaction. Therefore, it is the added chloride that creates a selective coupling catalyst leading to $C_3$-products and not a possible cation effect.

Table 1 also presents the results when 7.5 ml/min $CH_4$, 8.5 ml/min $O_2$ and 14 ml/min He are reacted over 0.6 g of $Na_2MoO_4$ and 0.6 g LiCl. Values for $SC_3$ up to 35% are noticed at 630°C with a concomitant $C_3$ yield of 2.8%. The combined $C_2$- and $C_3$-yields at 630°C turn out to be around 4.4%. The relatively high selectivities for $C_2$- and $C_3$-products observed below 650°C seem to be related to the fact that below this temperature, no significant CO evolution is observed. The $C_3$-product observed was around 20% of $C_3H_6$ and 80% of $C_3H_8$ at 620°C. The ratio of $C_3H_6/C_3H_8$ increased with temperature up to 1 : 1 at 690°C. Therefore, when using a catalyst, LiCl–$Na_2MoO_4$, different selectivities to $C_3H_6$ and $C_3H_8$ are observed as compared to the results obtained for an empty reactor. In the latter case, only $C_3H_6$ was observed. Addition of LiCl significantly increases $C_3$-selectivity, but hinders the conversion below the gas-phase level at $T > 610°C$. The main problem with molybdate catalyzed $CH_4$ coupling is the high yields observed for CO and $CO_2$ evolution, the total oxidation products [5–7,12–14]. It seems that up to 630°C, the catalytic centers in the $Na_2MoO_4$ + LiCl catalyst are involved in the generation of $C_2$- and $C_3$-products. Whilst the selectivity of the $C_3$-product increases, a concomitant decay in the selectivity of the $C_2$-product is observed.

From the data above 650°C shown in table 1, it is observed that by introducing a catalyst, LiCl–$Na_2MoO_4$, approximately only one half to two-third $CH_4$ conversion takes place as compared to that in an empty reactor. The addition of $Cl^-$ greatly reduces $CH_4$ conversion and, therefore, the total yield of higher hydrocarbon products, at these temperatures. In fact, above 650°C, the chloride poisons $C_3$ formation less than $C_2$, resulting in a net higher selectivity to $C_3$. It is also important to note that between 570 and 630°C, the methane conversion improved in the presence of $Na_2MoO_4$–LiCl catalyst when compared to that in an empty reactor and this is reflected in the higher $YC_2$ and $YC_3$ values. With only $Na_2MoO_4$ catalyst present, the $CH_4$ conversions were generally higher at all temperatures. However, no $C_3$-products were observed below 670°C. $Na_2MoO_4$ has low selectivity for $C_3$-products as seen in table 1. It melts at 687°C. The selectivity towards $C_3$-products when NaCl is added ($T > 670$°C) to $Na_2MoO_4$ goes up considerably. NaCl melts at 801°C. LiCl is used as a catalyst promoter because it is more covalent than NaCl. It melts as 610–614°C, indicating that liquid-phase LiCl on $Na_2MoO_4$ at temperatures around 600°C, favours the diffusion of $Cl^-$ in the molten state [23,24]. Concomitantly, the $SC_3$ values reported when using $Na_2MoO_4$ + LiCl as catalysts (table 2) increase under these conditions. The amounts of CO and $CO_2$ observed were lower in the presence of LiCl than in its absence, which is reflected in the increased values of $SC_2$ and $SC_3$ when LiCl is used, as seen in table 1. It seems that chloride incorporates on the host oxide lattice surface, either activating the surface or possibly producing defects in this surface. These defects would be created in the range of the reaction temperatures when LiCl is on the molybdate surface. At any rate, the chloride present is sufficient to modify the catalyst surface and create active and selective sites for $CH_4$ oxidation. This observation agrees with work recently reported by Burch et al. [14] on heterogeneous chlorine-promotion reactions in $CH_4$ activation.

$Mo^{6+}$–$O^-$ surface species can be produced by the dissociation of molybdates at the reaction temperatures used [5,6] and concomitant reduction of $Mo^{6+}$-ions by $CH_4$ [2–4]. The $Mo^{6+}$–$O^-$ surface species would then be the active centers involved

Table 2
XPS results showing surface concentrations of various elements (in at%) present in molybdate catalyst

| Element | $Li_2MoO_4$ | $Na_2MoO_4$ | $Na_2MoO_4$ + LiCl unreacted | $Na_2MoO_4$ + LiCl reacted 730°C/9 h | $Na_2MoO_4$ reacted 660°C/9 h |
|---|---|---|---|---|---|
| Na | traces | 12.7 | 4.46 | 3.80 | 5.54 |
| O | 46.1 | 43.5 | 9.00 | 12.3 | 14.8 |
| C | 40.6 | 33.9 | 55.7 | 34.2 | 50.9 |
| Mo | 10.4 | 9.83 | 0.53 | 1.04 | 0.86 |
| Cl | – | – | 28.1 | 38.5 | 24.3 |
| Li | 2.86 | – | 2.24 | 5.21 | 2.38 |
| Si | – | – | – | 5.1 | 1.2 |

in $CH_4$ oxidation on molybdate catalysts. This methyl radical formed during the reaction leads to the formation of $C_3$-products [4,25],

$$CH_3\cdot + C_2H_4 \rightarrow C_3H_7\cdot \rightarrow C_3H_6 + H\cdot \qquad (1)$$

and by radical recombinations,

$$C_2H_3\cdot + CH_3\cdot \rightarrow C_3H_6, \qquad (2)$$

$$C_2H_5\cdot + CH_3\cdot \rightarrow C_3H_8, \qquad (3)$$

$$C_3H_7\cdot + H\cdot \rightarrow C_3H_8. \qquad (4)$$

From the radical point of view [2–4], a mechanism involving the coupling of $CH_3\cdot + C_2H_3\cdot$ (vinyl) is possible, as shown by eq. (2) leading to the $C_3$-products. Alkali chlorides added would create acid centers in the catalyst and allow $CH_3\cdot + C_2H_4$ reaction [26,27]. Propane and propylene occurring in the reactions

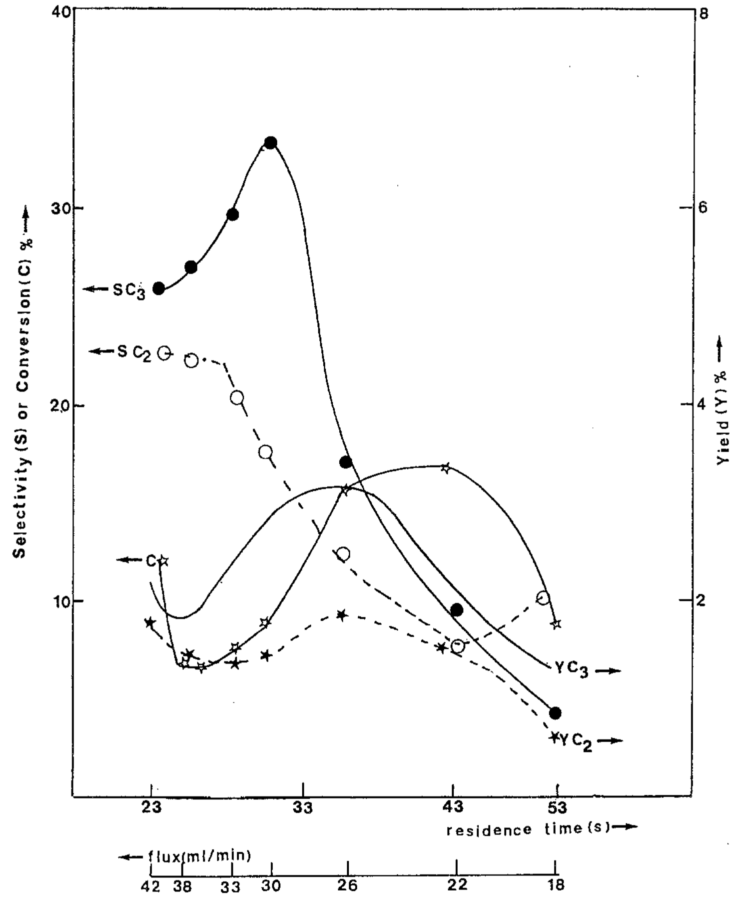

Fig. 1. Variation of selectivities and yields for $C_2$- and $C_3$-products as the total flux of $CH_4 + O_2 + He$ is varied at 620°C over 0.6 g of $Na_2MoO_4$ + 0.6 g of LiCl catalyst.

(eqs. (1)–(4)) due to the action of chloride containing catalyst may, under our specific experimental conditions, involve all these reactions simultaneously.

Fig. 1 shows the selectivities and yields of the products of $CH_4$ coupling when the total flux of gases is varied, conserving the ratio of $CH_4/O_2/He$ gas as used throughout in table 1. Reactions were carried out at 620°C. The decrease in $C_2$- and $C_3$-selectivity at lower flow rates is accountable to the fact that the contact time of the primary gases ($C_3H_6$ and $C_2H_4$) with the catalyst will be longer. This allows reaction of $C_3H_6$ and $C_2H_4$ with $O_2$ more readily, leading to CO, $CO_2$ and $H_2O$. It is to be noted that $CH_4$ conversion is not substantially changed by using a faster total gas flow. At low methane conversion, the $O_2$ remains at a relatively high concentration and the oxidation of the methyl radicals becomes more important compared with the coupling reaction. The adding of He reduces the residence time of the active gases $CH_4$ and $O_2$ and depresses the overall yields, but a higher selectivity for $C_2$- and $C_3$-products was observed in this case.

Fig. 2 shows the effects on $C_2$ and $C_3$ product formation when the ratio $R$ $CH_4/O_2$ is varied at 620°C in the $CH_4$ coupling reaction. It is readily seen that a

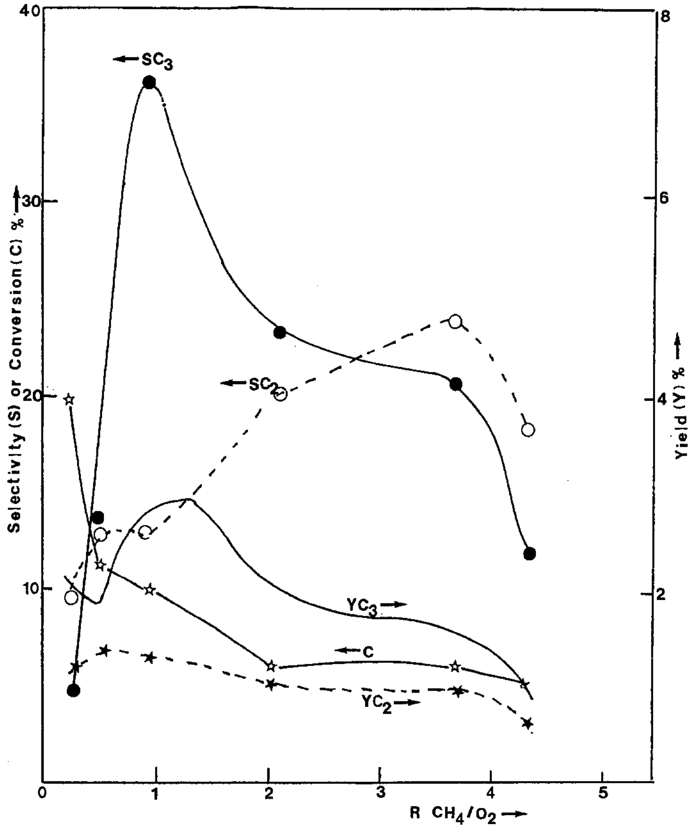

Fig. 2. Variation of selectivities and conversions for $C_2$- and $C_3$-products in $CH_4$ coupling at 620°C as a function of the ratio $CH_4$ to $O_2$ over a 0.6 g $Na_2MoO_4$ + 0.6 g LiCl catalyst.

ratio $CH_4/O_2$ somewhat below 1 affords the highest selectivity and yield for $C_3$-products. Assuming that methyl radicals are formed on the catalytic surface by dissociation of $CH_4$ and that these radicals fully react in the gas phase after desorption [2–4], two comments can be made on the experimental results observed in fig. 2:

(i) The high values of $SC_2$ observed when $CH_4$ is present in excess ($R$ $CH_4/O_2 > 1$), suggest that the amount of oxygenated radicals interacting with $CH_3\cdot$ leading to CO, $CO_2$ is low as compared to the $CH_3\cdot$ radicals present.

(ii) A high initial oxygen content, e.g., $CH_4/O_2 = 0.3$, favours the formation of $\cdot HO_2$, $\cdot OH$ and $\cdot O$ radicals, resulting in lower $SC_2$ and $SC_3$ values as seen in fig. 2 (left-hand side). Methane may be activated in the presence of $O_2$ as follows:

$$CH_4 + O_2 \rightarrow CH_3\cdot + \cdot HO_2, \tag{5}$$

$$CH_3\cdot + O_2 \rightarrow CH_2O + \cdot OH, \tag{6}$$

$$CH_3\cdot + O_2 \rightarrow CH_3O\cdot + \cdot O. \tag{7}$$

The influence of the reactions involving $\cdot HO_2$, $\cdot OH$ and $\cdot O$ should decrease with increasing $CH_4/O_2$ ratio because the oxygen concentration and, therefore, the concentration of oxygenated radicals reported in reactions (5), (6), (7), decreases.

Fig. 3a shows the Mo 3d X-ray photoelectron (XPS) measurements carried out on an unreacted $Na_2MoO_4 + LiCl$ sample. The same sample after reaction at 730°C for 9 h, is shown in fig. 3b. The spectra shown in figs. 3a and 3b have been obtained by subtraction of X-ray satellite peaks, and fit to a second-order polynomial according to ref. [28]. In fig. 3a, the narrow well defined peaks are indicative of one chemical state for the Mo (Mo VI) as seen from the shape of the doublet Mo 3d 5/2. The determination of the electrostatic charging of the catalyst samples was done by internal referencing to the contaminating aliphatic surface carbon at 284.6 eV, by cross checking the peak distances between C 1s, O 1s, Mo 3d 5/2 and Mo 3p 3/2 signals for the fresh and the reacted specimens, relative to pure standard samples of $MoO_3$ and by evaporating traces of gold onto the catalyst specimens and measuring the position of the Au signals. The quantitative results shown in table 2 indicate that on the surface of the $LiCl + Na_2MoO_4$ samples under the different experimental conditions used, a lot of chloride is still present. The quantitative determination of the elements as shown in table 2 has been referenced in the XPS-literature [29]. The surface enrichment of Si observed in the reacted catalyst is due to the contamination occurring from the attack of LiCl on the walls of the quartz reactor. Since the formation of $Li_2SiO_3$ indicates Li loss by the sample but the overall composition of the catalyst appears to be stable (table 2), this short time Li depletion would not be detectable due to the LiCl excess present as catalyst. Therefore, the overall surface of the catalyst would be stable, but a compensatory change is taking place on the catalyst. The formation of silicates was later verified in separate X-ray diffraction experiments. The surface concentration of C before

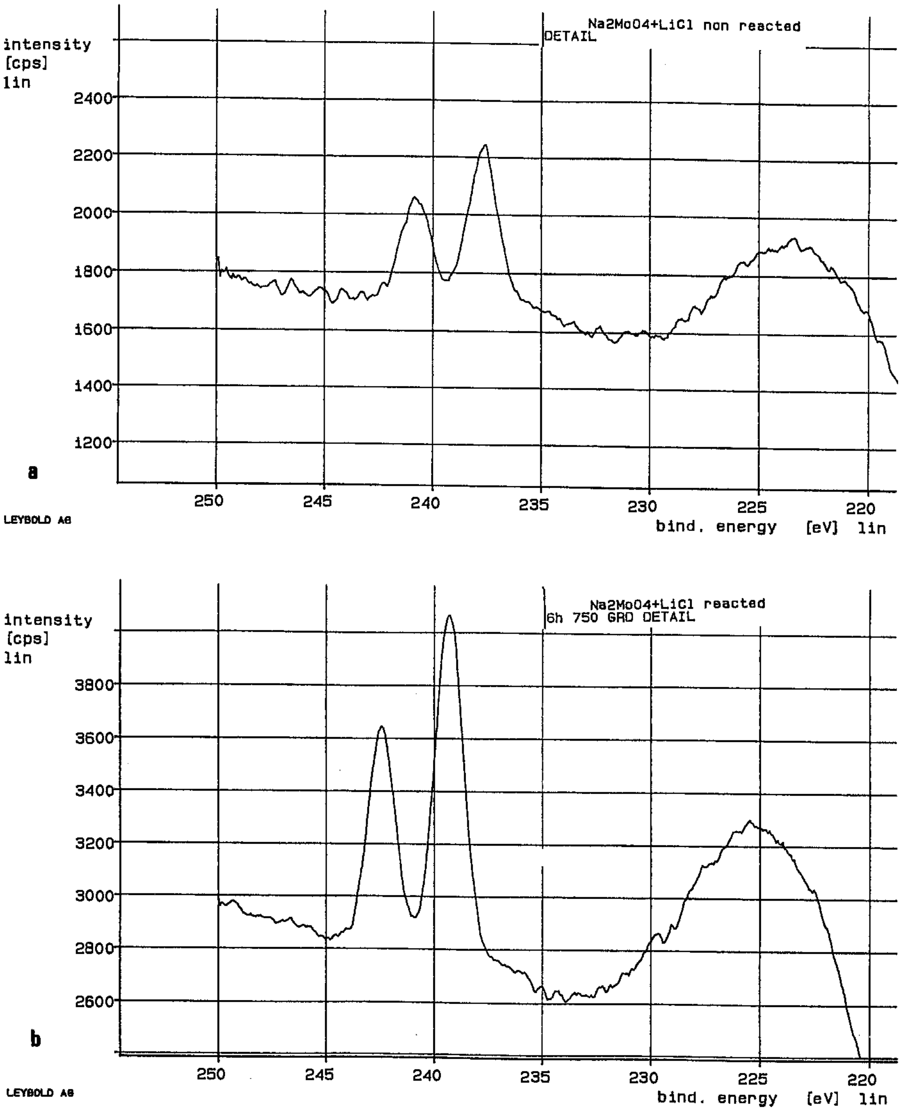

Fig. 3. (a) XPS spectra of the Mo 3d region for an unreacted $Na_2MoO_4$ + LiCl sample. Uncorrected spectra. (b) XPS spectra of the Mo 3d region for a $Na_2MoO_4$ + LiCl sample reacted at 730°C for 9 h. Uncorrected spectra.

and after reaction was nearly the same for all samples as shown in table 2. No C enrichment of the catalysts would be noticed during the reaction. The surface C present, reported by XPS is, therefore, derived out of the absorption from the atmosphere. The binding energy evaluation for the Mo 3d 5/2 doublet in table 2 was carried out according to refs. [30,31]. For the unreacted catalyst, the $Cl^-/Li$ observed ratio was 14/1 and not 1/1 (as seen in table 2) as stoichiometry suggests.

Table 3
Corrected binding energies for molybdate catalysts used

| Catalyst | Conditions | O (eV) | Mo (eV) |
|---|---|---|---|
| $Li_2MoO_4$ | unreacted | 530.6 | 232.7 |
| $Na_2MoO_4$ | unreacted | 530.3 | 232.3 |
| $Na_2MoO_4 + LiCl$ | unreacted | 530.9 | 232.7 |
| $Na_2MoO_4 + LiCl$ | 730°C/9 h | 531.1 | 232.4 |
| $Na_2MoO_4 + LiCl$ | 660°C/9 h | 530.8 | 232.4 |

This is due to the fact that an ideal stoichiometry can be detected by XPS only on clean, flat surfaces [28–31], not on rough irregular powdered type aggregates. Moreover, XPS measures the surface percentage of the atoms present in the upper layer. A high percentage of C (55.7%); O (9%); $Cl^-$ (28.1%); and Na (4.46%), proportionally cover most of the available catalyst [28], shielding the XPS surface signal. C sitting on Mo has previously been reported to produce shielding effects (when reporting surface enrichment) [30]. $Cl^-$ has a lower potential for surface deposition than cations such as Na, Mo, Li [29], and its relative surface density influences positively the intensity observed for this element by XPS signals.

Surface enrichment during the reaction for Mo (1.04% versus 0.53%) is reflected in fig. 3b by the relative magnitude of the peaks observed in the Mo 3d 5/2 doublet. Surprisingly, no distinct peak broadening is seen for the Mo 3d 5/2 doublet when comparing the unreacted and reacted samples in figs. 3a and 3b. Therefore, only one single valency state for Mo was found by XPS in both cases (Mo VI). Binding energy evaluation for the Mo 3d 5/2 signal after charging correction [28] was carried out for the different samples and is hereby reported in table 3. These signals indicate one singly valency state for Mo.

X-ray diffraction (XRD) was carried out for $Na_2MoO_4 + LiCl$ samples reacted at 660 or 730°C (9 h). Formation of up to 5.1% of $Li_2SiO_3$ was observed in the diffractogram, besides the typical spectra of $Na_2MoO_4 + LiCl$. This $Li_2SiO_3$ was formed when molten LiCl corroded the quartz reactor at the reaction temperatures. No additional phases were detected in the reacted $Na_2MoO_4$ by XRD technique. This is a proof that the catalyst is not affected during long-term catalysis.

## 4. Conclusion

The present work reveals that the direct formation of noticeable amounts of $C_3$-hydrocarbons during methane coupling is possible. This study presents in a phenomenological way the participation of $Cl^-$-ions in the formation of surface catalytic sites, which improve the $C_3$-selectivity during $CH_4$ coupling. The initial results obtained suggest that the role of chloride is complex. This study has shown that in this reaction, the adequate choice of catalyst material, temperature, residence time (high), reactant composition, dilution factor (low) and proper reactor design are important in achieving favourable $SC_3$ yields. In order to minimize gas-phase reactions during our work, the $CH_4$ and $O_2$ were diluted with He and a low $CH_4/O_2$ ratio was used.

## Acknowledgement

We thank Professor Guy-A. Martin for stimulating discussions in the course of this work.

## References

[1] G.E. Keller and M.M. Bhasin, J. Catal. 73 (1982) 9.
[2] G.J. Hutchings, M.S. Scurrell and J.R. Woodhouse, Chem. Soc. Rev. 18 (1989) 251.
[3] J.R. Anderson, Appl. Catal. 47 (1989) 177.
[4] J.C. Mackie, Catal. Rev. Sci-Eng. 33 (1991) 169.
[5] J. Kiwi, K.R. Thampi and M. Grätzel, J. Chem. Soc. Chem. Commun. (1990) 1690.
[6] J. Kiwi, K.R. Thampi, M. Grätzel, P. Albers and K. Seibold, J. Phys. Chem. 96 (1992) 1344.
[7] H. Matsuhashi, K. Sakurai and K. Arata, Chem. Lett. 4 (1989) 585.
[8] M. Baerns, Catal. Today 1 (1987) 357.
[9] J. Carreiro and M. Baerns, React. Kinet. Catal. Lett. 35 (1987) 349.
[10] J.M. Berty, Appl. Ind. Catal. 1 (1983) 207.
[11] C.F. Cullis, D.E. Keene and D.L. Trimm, J. Catal. 19 (1970) 378.
[12] R. Burch, G.D. Squire and S.C. Tsang, Appl. Catal. 46 (1989) 69.
[13] R. Burch, S. Chalker, G.D. Squire and S.C. Tsang, J. Chem. Soc. Faraday Trans. 86 (1990) 1607.
[14] R. Burch, S. Chalker and P. Loader, *Proc. Xth Int. Congr. on Catalysis*, Budapest 1992, pp. 8–17.
[15] D.C. Yates and N.E. Zlotin, J. Catal. 124 (1990) 562.
[16] M. Hatano, P. Hinson, K.S. Vines and J.H. Lunsford, J. Catal. 124 (1990) 557.
[17] Z. Kalenik and E. Wolf, J. Catal. 124 (1990) 566.
[18] G. Lane, E. Miro and E. Wolf, J. Catal. 119 (1989) 161.
[19] T.A. Garibyan and L.Ya. Margolis, Catal. Rev. Sci-Eng. 31 (1990) 355.
[20] E. Drauglis and R. Jaffe, *The Physical Basis for Heterogeneous Catalysis* (Plenum Press, New York, 1975).
[21] R. Busey and O. Keller, J. Chem. Phys. 41 (1964) 215.
[22] S.J. Korf, J.A. Roos, N.A. de Bruijn, J.G. van Ommen and J.R. Ross, J. Chem. Soc. Chem. Commun. (1987) 1433.
[23] T. Komatsu, T. Amaya and K. Otsuka, Catal. Lett. 3 (1989) 317.
[24] T. Ito, J.-X. Wang, C.-H. Lin and J.H. Lunsford, J. Am. Chem. Soc. 107 (1985) 5062.
[25] H. Zanthoff and M. Baerns, Ind. Eng. Chem. Res. 29 (1990) 2.
[26] V. Kazansky and B. Shelimov, Res. Chem. Interm. 15 (1991) 1.
[27] E. Tsang and P. Hampton, J. Phys. Chem. Data 15 (1986) 1087.
[28] A. Proctor and P. Sherwood, Anal. Chem. 52 (1980) 2315.
[29] C.D. Wagner, *Handbook of X-ray Photoelectron Spectroscopy* (Perkin Elmer, Phys. Elect. Div., Minneapolis, 1979).
[30] T.A. Patterson, J.C. Carrer, D.E. Leyden and D.M. Hercules, J. Phys. Chem. 80 (1976) 1700.
[31] S.O. Grim and L.J. Matienzo, Inorg. Chem. 14 (1975) 1014.